Optimal Synthesis of Stagewise Continuous Crystallization Process Networks

Ahmad Y. Sheikh and Alan G. Jones
Dept. of Chemical Engineering, University College London, London WC1E 7JE, U.K.

A new synthesis method based on targeting is presented for the design of stagewise continuous crystallization processes. The methodology determines the optimal flow distribution to each of the crystallizers in addition to other common control variables, including temperature, concentration, and vessel volume. The resulting optimization model yields a boundary-value differential equation system, which is transformed into a set of nonlinear equations through orthogonal collocation and solved numerically. For the synthesis of the continuous KNO_3 crystallization process considered here, the predicted optimal network solution shows that the common tradeoff between high yield and large average crystal sizes has been successfully eradicated by the new design approach.

Introduction

Continuous operation of mixed-suspension, mixed-product-removal (MSMPR) crystallizers, though beneficial in reducing capital and operating costs through smaller, less expensive equipment and reduced maintenance, is marked by some undesirable crystal product characteristics when compared with batch or classified-bed operation. None more so than the well-known exponential form of crystal size distribution (CSD), particularly when subsequent solid–liquid separation and most applications would desire a more uniform distribution. Process engineering solutions are therefore required.

A common approach for tackling this CSD problem is to design for poor mixing so that the resulting spatial CSD gradients can be exploited by fine-crystal dissolution and product classification loops. Such equipment is, however, difficult to design, requires abnormally high in-process inventories, and its operation is subject to cyclic behavior (Randolph and Tan, 1978). A series of MSMPR crystallizers in cascade offers a viable alternative that not only narrows the CSD, but also increases overall yield. This configuration also results in other improvements including flexible operation of temperature regimes, the possibility of using larger cooling surfaces and economies of energy consumption (Nývlt, 1992). On the debit side, however, it has been reported that cascaded design generally reduces the average crystal size when compared with an equivalent MSMPR crystallizer, and often these reductions outweigh the improvements in yield and the narrowed form of CSD (Randolph and Larson, 1988).

The performance of a cascaded crystallizer design is subject to operating temperature, feed concentration, crystal carryover from the previous stages, volume, and throughput for each crystallizer in the network. These variables have to be optimally determined to ensure that the main advantages of cascade configuration, such as increased yield and improved coefficient of variation, are not markedly offset by the undesirable attributes when compared with batch operation. The mathematical representation of such crystallization processes from a population balance results in an integro-partial differential equation that describes how the crystals are distributed by size and in time. This equation has to be solved along with the mass and energy balances to describe the complete process. In most situations of engineering interest—for instance, design and control—thorough knowledge of the CSD is unnecessary. Rather, some average quantities such as average size and coefficient of variation or other simplified description of the CSD is sufficient. The moment transform and analytical solution to the simplified population balance have emerged as the two common techniques to model the CSD within the crystallizers for stagewise processes (Hounslow and Wynn, 1992; Randolph and Tan, 1978).

The CSD performance in most studies has often been manipulated, however, by the characteristics of hydrocyclones that are frequently used in such systems. This has been mainly

Correspondence concerning this article should be addressed to A. G. Jones.
Current address of A. Y. Sheikh: G. D. Searle and Co., Skokie, IL 60077.

due to the use of simplified models used for crystallizers that do not provide many control variables having appreciable impact on the system performance. In the only significant attempt to design a stagewise process optimally (Larson and Wolff, 1971; reviewed in Randolph and Larson, 1988), the fractions of solute crystallized and crystallizer volumes were used as the control variables. Though effective in simplifying the models, these control variables, especially the fraction of solute crystallized, would be difficult to interpret physically during the design. It has also been observed that such studies often exclude energy balances from the models. The latter are of paramount importance, however, because economy of energy consumption is a very important feature of stagewise processes. Besides, an overall optimal solution to the complete synthesis problem can only be achieved if as many subsystems as possible are considered simultaneously.

The network structures considered heretofore are very rigid in that only simple cascade configurations are modeled (Randolph and Tan, 1978). Optimal design based on alternative flow by, for example, feed stream bypass and intermediate product removal, together with the choice of different crystallizer types and the other common control variables, holds the potential for extending the performance currently achieved from stagewise processes. This strategy would not only affect crystal carryover, but also supersaturation levels within the vessels through mixing and hence affect product CSD.

Despite recent advances in crystallization process simulations (Hill and Ng, 1997; Hounslow and Wynn, 1993) and the upsurge in advanced strategies for reactor network synthesis, no prior work has been reported on stagewise crystallization that exploits modern strategies. An extensive review of these new approaches can be found in Hildebrandt and Biegler (1995). One such technique for the synthesis of reactor networks is the "targeting" method due to Balakrishna and Biegler (1992a). The targeting-based techniques have not only been extensively refined for the chemical reactors (Balakrishna and Biegler, 1992a,b, 1996), but also effectively applied to the synthesis of azeotropic distillation networks (Doherty et al., 1985). It finds its origins in the pinch technology for heat-exchanger networks (Linhoff and Hindmarsh, 1983). The method exploits physical and geometric insight of the system to predict *a priori* certain features that an optimal or feasible solution should reflect. With the method only providing the guidelines, that is, the targets, the search for the optimal solution is carried out through rigorous models representing the components of the network that are sequentially solved through the nonlinear programming techniques. These procedures for chemical reactors can be modified to account for the peculiarities of crystallization processes that arise from the incorporation of the CSD description through careful modeling.

In the present work, an optimization problem based on the targeting approach will be developed for the synthesis of stagewise crystallization processes. The constructive nature of the targeting methodology results in the sequential solution of small nonlinear programs, which are well suited for developing models comprising mass balances, population balances, and highly nonlinear expressions for nucleation and growth rates. First the basic reactor model for chemical reactor networks due to Balakrishna and Biegler (1992a) will be briefly reviewed. This review will be followed by the derivation of the optimization problem for a crystallization system and its mathematical transformation into a solvable form. In the next section, a rigorous model based on the analytical solution to population balance will be presented for thorough analysis of the optimal solution. Finally, process synthesis of KNO_3 crystallization will illustrate the methodology, conclusions will be drawn, and possible future directions of this work discussed.

Targeting Method for Chemical Reactors

The synthesis of reactor networks is based on mixing between different reacting environments and proceeds by determining the maximum possible performance through reaction and mixing without explicitly specifying the network structure. A network capable of achieving this target is then devised by extending the concept of attainable regions, using simple optimization formulations. The segregated flow (SF) reactor model (Balakrishna and Biegler, 1992a) works at the heart of the targeting approach because it is often sufficient to establish performance bounds for isothermal processes, particularly when the concentration of product species is a concave function of reactant concentration (Glasser et al., 1987). In SF models (representing both plug-flow reactors (PFR) and PFR with bypasses), only molecules of the same age are well mixed, while mixing between molecules of different ages takes place at the exit. Even when the concavity condition is not satisfied, as when it is possible to extend performance beyond the levels predicted by the SF solution, these models can be used in conjunction with small nonlinear programs for recycle reactor extensions to improve the objective function.

The extension of the SF model to nonisothermal systems, however, requires redefinition of the entire reactor model because the SF structure assumes negligible costs of mixing. In the nonisothermal case this translates as zero cost of maintaining the temperature profile. For such processes, Balakrishna and Biegler (1992b) developed a cross-flow reactor (CFR) model that is not only capable of allowing temperature manipulations through feed mixing and external heating or cooling but for some systems also precludes the need to check for reactor extensions. Figure 1 shows a CFR model. At one extreme, when $q(\alpha)$ is zero for a general value of $f(\alpha)$, the model reduces to a completely segregated flow system, while a maximum mixed model is obtained for a general

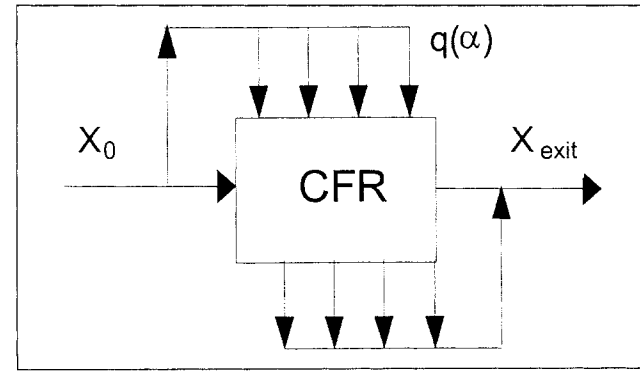

Figure 1. Cross-flow reactor model (Balakrishna and Biegler, 1992b).

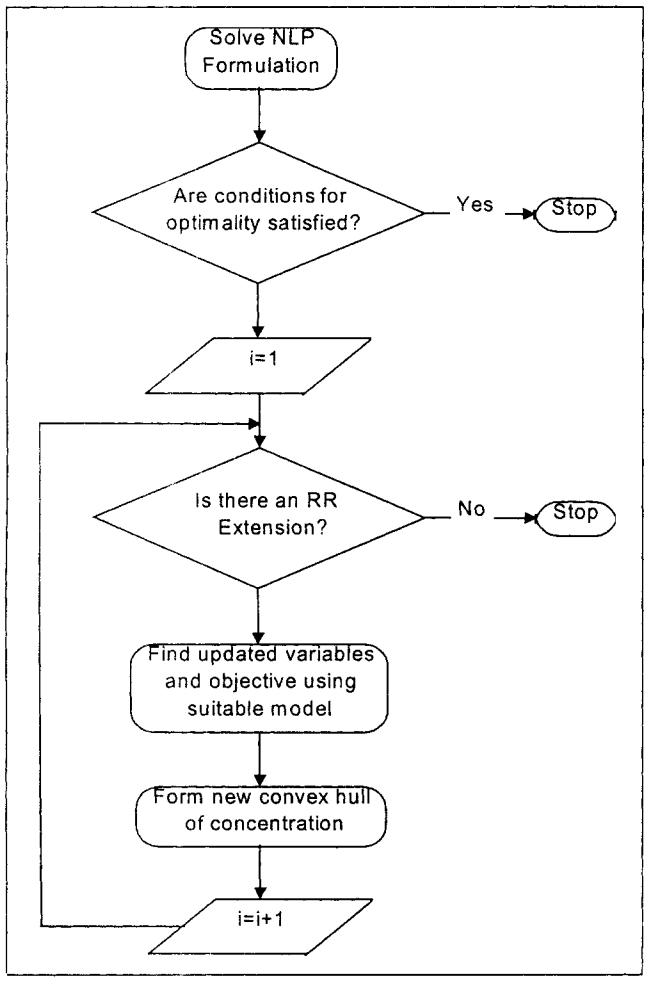

Figure 2. Constructive procedure for reactor network synthesis using targeting procedure.

nonzero $q(\alpha)$ and $f(\alpha)$ as a Dirac delta function at exactly one point. The model results in a dynamic optimization problem where temperature, feed distribution, and exit flow distribution functions are the control profiles. The concavity conditions are applicable if the temperature profile can be related to the concentration profile (e.g., adiabatic reactors). More general nonisothermal reactors with arbitrary temperature profiles, however, require a sequential procedure (see Figure 2) where recycle reactor extensions are checked after solving the CFR model. The procedure is repeated until no improvements in the objective function are observed.

The mathematical details of the different reactor models used by the constructive targeting methodology can be found in Balakrishna and Biegler (1996). The technique has been coupled with the energy integration and separation sequences with relative ease (Balakrishna and Biegler, 1996) to provide a comprehensive framework for integrated design.

Problem Formulation for a Crystallizer Network

In the context of stagewise crystallization, the CFR structure is not only desirable for energy integration, but also because it provides controls to manipulate the crystal carryover and even supersaturation levels through the side streams. Full carryover from stage to stage is one of the major contributors to the diminishing levels of supersaturation in simple cascades that result in markedly reduced average crystal size.

The moment transformation will be used to obtain a lower dimension formulation of the population balance that converts it into a set of ordinary differential equations, with the first four related to total number, length, area, and volume of crystals, respectively. These equations have to be added to the general CFR model due to Balakrishna and Biegler (1992b). The other major difference between crystallization and common chemical reactions is that in the former two kinetic processes occur simultaneously, namely, nucleation of crystals and their subsequent growth. Furthermore, the opposite relationship between average size and yield, apparent from the comparison of MSMPR crystallizer and simple cascade performances, has to be incorporated into the objective function.

Model development for the boundary-value problem

The optimal control problem based on the CFR model can be developed for crystallizers in a dimensionless form with the moment balances as follows:

$$\max_{q(\alpha),f(\alpha),T(\alpha)} \quad J(X_{\text{exit}}, \tau, L_{\text{av}})$$

$$\frac{dX}{dt} = -3\frac{k_v}{k_a}\bar{A}G + \frac{q(\alpha)Q_0}{Q(\alpha)}[X_0 - X(\alpha)] \tag{1}$$

$$\frac{dn}{dt} = \frac{q(\alpha)Q_0}{Q(\alpha)}B \tag{2}$$

$$\frac{dL}{dt} = nG \tag{3}$$

$$\frac{d\bar{A}}{dt} = 2k_a LG \tag{4}$$

$$L_{\text{av}} = \int_0^\infty f(\alpha)L(\alpha)\,d\alpha \Big/ \int_0^\infty f(\alpha)n(\alpha)\,d\alpha \tag{5}$$

$$B = A\exp\left(-c\Big/\left\{T^3\left[\ln\left(\frac{X}{X_{\text{sat}}(T)}\right)\right]^2\right\}\right) \tag{6}$$

$$G = k_g[X - X_{\text{sat}}(T)] \tag{7}$$

$$X_{\text{exit}} = \int_0^\infty f(\alpha)X(\alpha)\,d\alpha \tag{8}$$

$$\int_0^\infty \int_0^\alpha [q(\alpha') - f(\alpha')]\,d\alpha'\,d\alpha = \tau \tag{9}$$

$$\int_0^\infty f(\alpha)\,d\alpha = 1.0 \tag{10}$$

$$\int_0^\infty q(\alpha)\,d\alpha = 1.0 \tag{11}$$

$$Q(\alpha)/Q_0 = \int_0^\alpha (q(\alpha') - f(\alpha'))\,d\alpha'. \tag{12}$$

The independent variable is restricted to a maximum value of 1 and so is the state "X" at the first boundary. The first four equations define differential solute mass and crystal moment balances, while Eqs. 6 and 7 couple them through kinetic expressions. The optimal solution to this boundary-value problem that maximizes J, provides a lower bound on performance by simultaneously considering the relevant properties of CSD along with the yield.

Model transformations using orthogonal collocation

Common adjoint techniques can be used to solve the preceding differential algebraic equation (DAE) optimization problem. Orthogonal collocation on finite elements has, however, emerged as the preferred discretization technique (Cuthrell and Biegler, 1987), for it leads to solutions that are easier to interpret physically. Furthermore, the integrals within the problem are automatically evaluated at Gaussian quadrature points. These features, along with the fact that state constraints can be imposed directly, are very important within the context of the synthesis problem, for they allow the use of continuous-stirred-tank-reactor (CSTR)-type rate equations in the differential mass balance (Cuthrell and Biegler, 1987). These properties are even more significant to the crystallization model because integrated forms of the analogous continuous MSMPR-type equations of the differential moment balances (Eqs. 2–4) can be used within the collocation points to calculate the rate of solute loss.

Figure 3 shows the equivalent discretized CFR environment, where state equations are optimally solved at collocation points within the finite elements. The following simplified nonlinear program can be developed to find optimal performance by orthogonal collocation on finite elements with Lagrange interpolation functions:

$$\max_{q_i, f_{ij}, T_i} \quad J(X_{\text{exit}}, \tau, L_{\text{av}})$$

$$\sum_k X_{ik} L'_k(\alpha_{ij}) - R(X_{ij}, T_i)\Delta\alpha_{ij} = 0 \tag{13}$$

$$\left[n_{ij} = B_{ij}(\alpha_{ij} - \alpha_{ij-1})Q_{ij}\right] + \left\{\left[1 - \left(\frac{f_{ij-1}}{Q_{ij-1}}\right)\right] \times n_{ij-1}\right\} \tag{14}$$

$$L_{ij} = n_{ij} G_{ij} \tau_{ij} + \left\{\left[1 - \left(\frac{f_{ij-1}}{Q_{ij-1}}\right)\right] \times L_{ij-1}\right\} \tag{15}$$

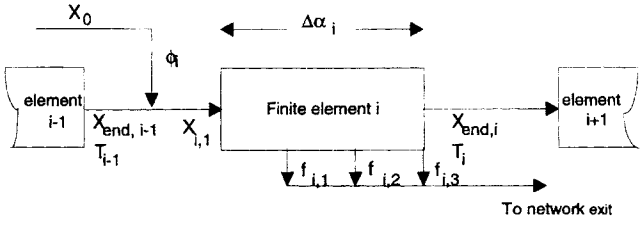

Figure 3. Discretized CFR model for nonisothermal synthesis.

$$A_{ij} = L_{ij} G_{ij} \tau_{ij} + \left\{\left[1 - \left(\frac{f_{ij-1}}{Q_{ij-1}}\right)\right] \times A_{ij-1}\right\} \tag{16}$$

$$R(X_{ij}, T_i) = A_{ij} G_{ij} \tau_{ij} \tag{17}$$

$$L_{\text{av}} = \frac{\sum_i \sum_j L_{ij} f_{ij}}{\sum_i \sum_j n_{ij} f_{ij}} \tag{18}$$

$$B_{ij} = A \exp\left(-c \Big/ \left\{T^3 \left[\ln\left(\frac{X_{ij}}{X_{\text{sat}}(T_i)}\right)\right]^2\right\}\right) \tag{19}$$

$$G_{ij} = k_g\left[X_{ij} - X_{\text{sat}}(T_i)\right] \tag{20}$$

$$X(0) = X_0 \tag{21}$$

$$X_{i,0} = \phi_i X_0 + (1 - \phi_i) X_{i-1,\text{end}} \tag{22}$$

$$X_{i,\text{end}} = \sum_k X_{ik} L_k(\alpha_{i+1,0}) \tag{23}$$

$$X_{\text{exit}} = \sum_i \sum_j X_{ij} f_{ij} \tag{24}$$

$$n_{\text{exit}} = \sum_i \sum_j n_{ij} f_{ij} \tag{25}$$

$$\tau = \sum_i \sum_j \alpha_{ij}(q_i - f_{ij}) \tag{26}$$

$$Q_{ij} = \sum_i \sum_j (q_i - f_{ij}) \tag{27}$$

$$\phi_i = Q_{i,0}/Q_{ij} \tag{28}$$

$$\sum_i q_i = 1.0 \tag{29}$$

$$\sum_i \sum_j f_{ij} = 1.0. \tag{30}$$

The discretized differential solute balance at the jth collocation point in the ith finite element is represented by Eq. 13. Equations 14–16, the constituents of the rate of solute removal due to crystallization (Eq. 17), are dimensionless analogs of zeroth, first, and second moments of CSD in integrated form. The second terms in these equations manifest the effects of crystal carryover from the previous intervals. The balance between feed and crystallizing streams is represented by Eq. 22, while Eqs. 29 and 30 are the discretized forms of Eqs. 10 and 11 obtained through Gaussian quadrature. The values of state variable X in an element are extrapolated to find its magnitudes at the end through Eq. 23. The collocation points are optimally selected as roots of a Jacobi polynomial of an equivalent order.

This discretized model only solves the solute balance through interpolation functions, because the ability to use the integrated form of moment balances between collocation points eliminates the need for a similar representation of the differential moment balances. As a result the problem is greatly simplified. It would, however, require a large number of points for a satisfactory solution. These are not only needed for the validity of MSMPR-type equations between the points,

but also for mathematical reasons stemming from highly nonlinear discontinuous equations within the problem.

Descending temperature profiles are often used in stagewise crystallization to compensate reductions in supersaturation levels (Nývlt, 1992). This relationship between temperature and concentration satisfies the modified sufficiency condition to interpret CFR-type solution as optimal for any concave objective function. The need to check for recycle extensions is therefore eliminated. This is not to suggest, however, that the constructive approach (Figure 2) should not be used to find more complex networks using arbitrary temperature profiles.

Implementation details and solution technique

General performance specifications for stagewise systems do not exist in terms of CSD parameters, and therefore the objective functions for such problems often depend on the end use envisaged for the product. In this work, a composite objective function comprising yield and average size is developed to penalize the total number of crystals.

Twenty collocation points over five equisized finite elements (same $\Delta\alpha$) are used during discretization. The value of temperature drops from 291 K to 288 K over these elements. The actual drop from one element to the next (not shown) is calculated (Sheikh, 1997) by a theoretical equation given by Nývlt (1992). Cooling crystallization of potassium nitrate is selected for illustration due to its relatively well-established kinetics and moderate temperature dependence of solubility. The kinetic parameters are appropriately scaled to determine the coefficients for nucleation and growth-rate expressions in the dimensionless optimization problem. The problem is simplified by calculating nucleation rate (Eq. 19) from the entry-level concentration into the elements instead of its local point value. This will overpredict the number of crystals. With all the variables normalized and retention times very small, however, the effect on diminutive changes in dimensionless yield is not expected to be significant. A maximum of 0.6 is imposed on both q_i and f_{ij} to ensure a more even distribution of flow within the elements.

The nonlinear program (NLP) is solved using the sequential quadratic programming (SQP) algorithm because the dimension of the problem is relatively small (number of equations < 100) and it comprises highly nonlinear constraints appearing as discretized state equations. Furthermore, the convergence is quadratic and, unlike the reduced-gradient method without restoration (MINOS), the method does not require linearization of active constraints around the starting points.

Rigorous Models for Complete Crystal Size Distribution

The simplified nondimensional nature of the preceding optimization problem necessitates the development of rigorous models for detailed analysis and comparison of its findings. The model reported below is based on the analytical solution to a simplified population balance that ignores effects of crystal agglomeration and disruption. It provides complete CSD in each crystallizer and does not suffer from errors in mass balances, often observed in discretized solutions (Lister et al., 1995). The simple population balance representing number flow for the ith stage takes the following general form (Hounslow and Wynn, 1992):

$$\frac{\partial n_i}{\partial L} = \frac{n_{i-1} - n_i}{G_i \tau_i},$$

subject to

$$n_i(0) = \frac{V_i B_i^0}{G_i \tau_i}. \tag{31}$$

This steady-state form is amenable to analytical solution, and the application of an integrating factor followed by subsequent integration yields

$$n_i(L) = \exp\left(\frac{-L}{G_i \tau_i}\right)\left(\frac{V_i B_i^0}{G_i \tau_i} + \int_0^L \frac{n_{i-1}}{G_i \tau_i} \exp\left(\frac{L}{G_i \tau_i}\right) dL\right). \tag{32}$$

For its solution, an empirical linear crystal-growth-rate expression is used together with an approximate primary nucleation-rate expression. The latter not only helps simplify the problem by eliminating the nucleation-rate dependence on crystal mass (Sheikh and Jones, 1997), but also provides a good test of robustness for the SQP algorithm through its highly nonlinear form:

$$B = 1.8 \times 10^{16} \exp\left(\frac{-0.5}{[\ln(s)]^2}\right) \tag{33}$$

$$G = 2.27 \times 10^{-5} [X - X_{\text{sat}}(T)]. \tag{34}$$

Kinetic parameters in these equations are taken from Mullin (1993) with the coefficients based on rates expressed in $\text{cm}^{-3} \cdot \text{s}^{-1}$ and $\text{cm} \cdot \text{s}^{-1}$, respectively (temperature dependence could be included in the general case but is neglected here). These equations (Eqs. 32–34) will be solved in conjunction with the appropriately defined mass balance to simulate five MSMPR crystallizers, each designed according to the specifications determined from the NLP for the five finite elements. Details of the general modeling framework used here can be found in Sheikh and Jones (1997). Though adequate for illustration purposes, these simulations will be a simplified representation of the optimal solution, because the latter employs MSMPR-type approximations for crystallization rate between collocation points and not over the elements.

Optimal Configuration and Its Analysis

The results from the optimization program and its detailed simulation are presented in the following sections. Comparisons with other possible configurations are used to analyze the findings.

Nonlinear program

The solution to the NLP representing crystallizer synthesis model determined an optimum configuration with dimension-

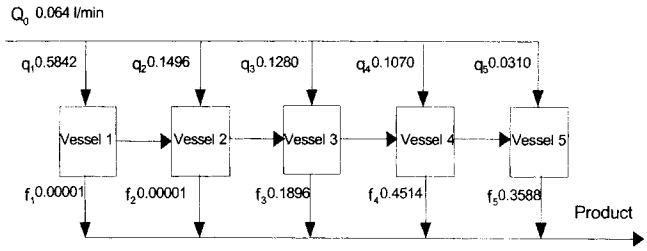

Figure 4. Optimal flow profiles for KNO_3 crystallization-process network.

less yield, average crystals size, and CV of 0.3749×10^{-3}, 0.1157×10^{-3}, and 0.6654, respectively. (Note that the coefficient of variation for ideal MSMPR crystallizers is 1.0 here rather than the more usual 0.5 because the moments are calculated on the basis of number flow rather than density.) This solution represents the best compromise between two extremes in design, namely, MSMPR and simple cascade. The former provides the largest average sizes and coefficient of variation at a reduced yield, while the reverse is true for simple cascade (Larson and Wolff, 1971). Flow distribution of each finite element within the optimal network is depicted in Figure 4. Since no experimental or simulated data are available, three other design configurations with similar characteristics (designs involving flow distribution) were developed to compare and analyze the performance of the optimal network. The cases include:

1. Descending temperature profile and same flow distribution for all the finite elements (q_i and f_i equal to 0.2 throughout)
2. Constant temperature and optimal flow distribution as determined by the NLP
3. Constant temperature and same flow distribution.

Table 1 depicts predictions for the three criteria variables from different schemes. It can be seen that it is possible to improve CV by operating at constant temperature (cases 2 and 3). Average size can also be increased when optimal flow distribution is used in conjunction with constant-temperature profile (case 2). These improvements could be due to the shift of reduced supersaturation toward crystal growth. None of the schemes, however, succeed in improving the yield beyond the levels obtained from optimal solution. The latter outperforms case (1), which only differs from it in flow distribution in all three criteria.

Detailed simulations of the network

In this section, results from detailed simulations of the optimal network comprising five MSMPR-type crystallizers are

Table 1. Case Studies Results for Crystal Yield, Average Size, and CV

Case	Yield (Dimensionless)	Avg. Crystal Size (Dimensionless)	Coeff. of Variation
Optimal solution	0.3749×10^{-3}	0.1157×10^{-3}	0.6654
a	0.2508×10^{-4}	0.6468×10^{-4}	0.7375
b	0.7676×10^{-5}	0.2267×10^{-3}	0.6382
c	0.3666×10^{-6}	0.9328×10^{-4}	0.6121

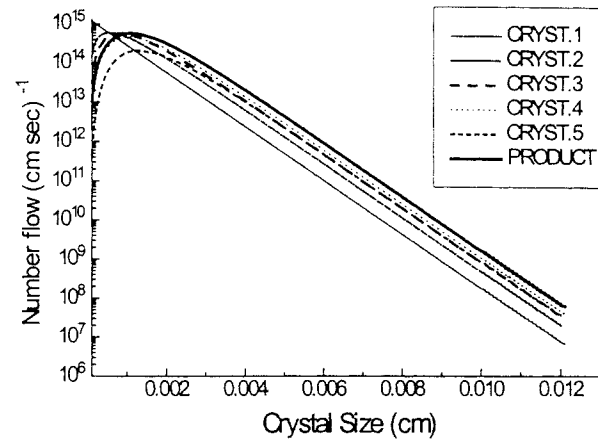

Figure 5. Crystal size distributions from each crystallizer and product stream.

reported. The findings are compared with equivalent MSMPR crystallizers and a simple cascade. Finally the performance of the optimal network is quantified at higher levels of supersaturation.

Each crystallizer has a volume of 9.07 m^3, while the feed concentration is 3.52 $kmol\cdot m^{-3}$ and the same temperature profile as in the NLP is used. The total flows (fresh feed plus stream from the preceding crystallizer as determined from the NLP) to each vessel are 0.13668, 0.17168, 0.20163, 0.1826, and 0.0889 $m^3\cdot s^{-1}$, respectively. It is worth noting that these optimally determined flow rates, if transformed into variable vessel volumes, would show that the volume of individual crystallizers increases down the network. This observation is in line with the general findings of chemical-reaction engineering, which suggest a similar configuration for higher order reactions (Levenspiel, 1972). A check on the levels of supersaturation indicates that they drop along the network to such extents that nucleation is only significant in the first vessel, following which crystal growth predominates. Consequently, the numbers of crystals do not increase significantly, while the growth rate steadily drops. Figure 5 shows predicted CSD in the crystallizers and the product stream. The shape of product CSD shows all the attributes of a system where not all the small crystals stay in the reacting environment for the same average retention time (Randolph and Larson, 1988). The fact that nucleation virtually ceases after the first stage can also be observed from Figure 5. In Figure 6, normalized CSD for the five vessels are plotted to qualitatively present the effect of staging. It can be seen that as the system progresses down the network, the peaks in CSD shift to the right and the symmetry of the distribution deteriorates. The markedly reduced heights of curves 4 and 5 reflect significant reductions in the number of crystals within the system due to intermediate product removal. It can also be inferred that the average size of the product stream lies between the sizes from crystallizers 4 and 5.

Figure 7 compares crystal size distributions from the optimal network to those obtained from a similar simple MSMPR cascade and two single MSMPR crystallizers. The details of other variables are listed in Table 2. The single crystallizers have the same volume and throughput as the total volume and throughput in the optimal network and simple cascade.

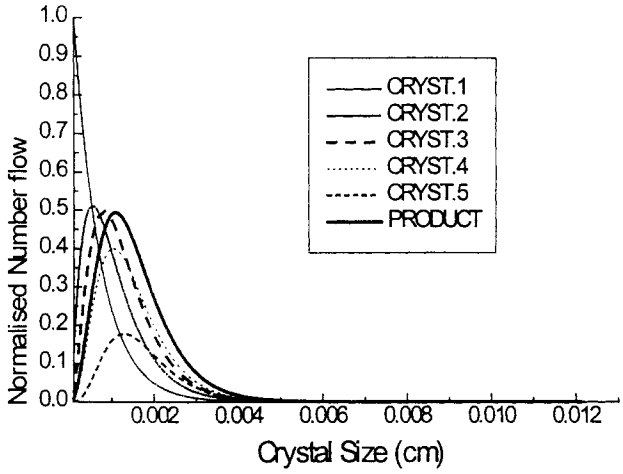

Figure 6. Normalized CSD from the optimal network.

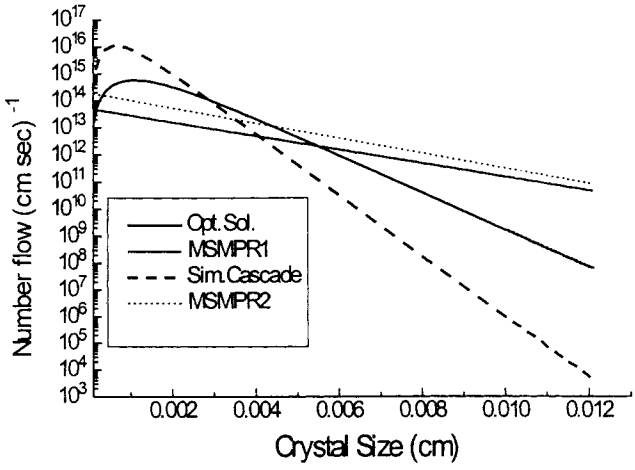

Figure 7. Product CSD from optimal crystallizer network, simple cascade, and MSMPR.

Each of these operates at the extremes within the temperature profile used for the optimal network and simple cascade and the optimum would therefore lie between these two crystallizers. It is worth noting that the exit streams from the optimal and simple cascade design are not at the same temperature, the former being the weighted-average of the temperatures in each crystallizer, while the latter is the temperature of the final crystallizer.

The results indeed confirm that the optimal solution performs between the cascade and single crystallizers. It succeeds in increasing the yield by 280% when compared with the single crystallizer operating at the higher temperature (MSMPR 1) for a 17% reduction in average size. Though the yield is only up 115% on the single crystallizer operating at the lower temperature (MSMPR 2), it also accompanies reductions in the degradation of average size (to ~8%). The simple cascade achieves 365 and 145% higher yield for 54 and 45% reductions in average size when compared with MSMPR 1 and 2, respectively. The magnitudes of the reductions in average sizes and coefficient of variation observed here for the simple cascade are comparable to those obtained from the simple calculation methods cited by Mullin (1993) for such designs.

The exit concentration from the first vessel in simple cascade is higher than that from the optimal network. The nucleation rate is, therefore, greater, which is reflected in Figure 7 through a larger number of small crystals. This low initial conversion in the simple cascade is a direct consequence of the fact that the entire feed is fed in a vessel of similar volume. The steeper slope manifests the effects of full crystal carryover from stage to stage that relieves supersaturation at a faster rate and consequently lower growth rates when compared with the optimal solution. The MSMPR crystallizers provide the best average size because the mean residence time is much higher.

Significant differences in average size and coefficient of variation between the optimal network and simple cascade

Table 2. Average Size, CV, Yield, and Exit Concentration from Different Crystallizer Environments

	Crystallizer 1	Crystallizer 2	Crystallizer 3	Crystallizer 4	Crystallizer 5	Product
Optimal solution						
C_out kmol·m^{-3}	3.318	3.165	3.018	2.871	2.669	2.827
Overall yield (%)	—	—	—	—	—	19.6
CV	1.000	0.727	0.617	0.545	0.487	0.512
LBAR cm	6.30×10^{-4}	1.02×10^{-3}	1.26×10^{-3}	1.49×10^{-3}	1.74×10^{-3}	1.61×10^{-3}
Simple cascade						
C_out kmol·m^{-3}	3.337	3.111	2.933	2.778	2.644	2.644
Overall yield (%)	—	—	—	—	—	24.8
CV	1.000	0.726	0.622	0.562	0.523	0.523
LBAR cm	3.83×10^{-4}	6.20×10^{-4}	7.58×10^{-4}	8.57×10^{-4}	9.32×10^{-4}	9.32×10^{-4}
MSMPR 1 (Temperature 291 K)						
C_out kmol·m^{-3}	—	—	—	—	—	3.281
Overall yield (%)	—	—	—	—	—	6.6
CV	—	—	—	—	—	1.000
LBAR cm	—	—	—	—	—	1.93×10^{-3}
MSMPR 2 (Temperature 288 K)						
C_out kmol·m^{-3}	—	—	—	—	—	2.918
Overall yield (%)	—	—	—	—	—	17.1
CV	—	—	—	—	—	1.000
LBAR cm	—	—	—	—	—	1.74×10^{-3}

Table 3. Moments for the Optimal Network and Simple Cascade

Crystallizer	Moment 0 ($\times 10^{-6}$ cm^{-3})	Moment 1 ($\times 10^{-6}$ cm·cm^{-3})	Moment 2 ($\times 10^{-6}$ cm^2·cm^{-3})
Optimal network			
1	6,403,765.6	4,036.85	5.089533
2	5,098,058.9	5,181.95	5.052975
3	4,340,749.2	5,474.86	9.537487
4	3,619,397.0	5,415.80	10.4402
5	3,206,364.8	5,830.89	12.5756
Simple cascade			
1	25,786,219.2	9,898.68	7.59975
2	25,786,219.2	16,010.93	15.1900
3	25,786,219.2	19,561.13	20.5763
4	25,786,219.2	22,117.11	24.9609
5	25,786,219.2	24,056.87	28.5802

can be explained by analyzing the moments within each environment. These are listed in Table 3 in their conventional dimensions. In the optimal design the number of crystals (zeroth moment) continually drops not only due to the increasing flow rates into the vessels that do not accompany new crystals but also because the intermediate product removal becomes significant. The first and second moments, however, continually increase, with the exception of fourth vessel, where the first moment shows a drop. The reason for this could be that the increase in its magnitude due to growth fails to compensate for very low number density as the ratio of fresh feed to carryover reaches its maximum value. These moment trends are in sharp contrast to those observed in a simple cascade where the zeroth moment remains constant while the others continually increase. While longer residence time in the first vessel within the optimal network could also contribute to significantly higher average sizes, CV is greatly affected by the changes in moments resulting from flow distribution. The first two vessels in both the cascade and the optimal network operate in an identical manner since insignificant amounts of product are withdrawn from the first vessel in the optimal configuration. This can be observed from the near identical values for CV in both the environments up to the second vessel. As the flow patterns and consequently the trends in moments start to diverge, however, CV drops more rapidly in the optimal network. Hence the optimal solution outperforms simple cascade in both the attributes of the CSD considered in the present model.

The performance of optimal network is also studied at very high supersaturation throughout the network achieved by lowering the vessel temperatures. Though the resulting network is no longer optimal, because the NLP finds the optimum using supersaturation levels, it is nevertheless considered worthwhile to analyze the system with significant nucleation in each vessel. In Figure 8, product CSD from such a design is compared with a similar simple cascade and the earlier findings. It can be seen that the new solution still outperforms a similar simple cascade. The magnitude of improvements in average size is, however, significantly reduced. This is not only due to the reduction in sizes for the network based on the optimal configuration resulting from an increase in the number of crystals but also because the average size from the simple cascade increases. The latter could be attributed to the fact that nucleation diminishes earlier in such a design, leaving the driving force mainly for crystal growth.

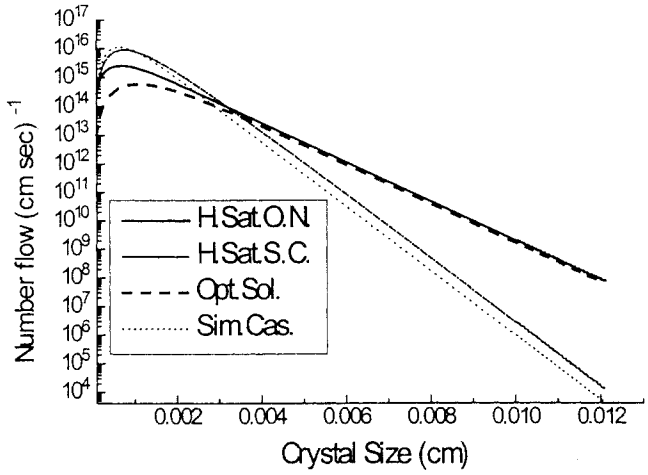

Figure 8. CSD from high supersaturation analogs of optimal network and simple cascade.

Conclusions

In this work a targeting-based method is developed for optimal synthesis of stagewise crystallization process networks. The methodology draws its structure from a similar approach developed by Balakrishna and Biegler (1996) for chemical reactor networks. It provides an optimization-based method for trading between maximum yield (simple cascade) and best average size (MSMPR) by fundamentally changing the characteristics of stagewise design through innovative flow distributions. The procedure has been demonstrated for a KNO_3 crystallization process. For the conditions used in the simulations of optimal network, an increase of more than 115% is achieved in yield when compared with the best performing MSMPR (yieldwise) of similar volume and throughput at the expense of at the most a 17% reduction in average size (best MSMPR, average sizewise). Though higher yield (340%) can be obtained from a simple cascade, the degradation of average size is more pronounced (~ 50% reduction on the size from a single MSMPR). The coefficient of variation is also reduced to a greater extent in the optimal design.

Despite the fact that the magnitudes of these results are strongly related to the kinetics and temperature profiles, the methodology is of more general utility. The optimal configuration will inherently result in more efficient networks. This is because the provision of side feeds not only eliminates the need for equal volumes/flow rates of each crystallizer but also reduces the energy requirements for cooling the suspension, since mixing of the feed and crystallizing streams itself increases solute concentration.

A large number of collocation points have been found to be essential for an acceptable numerical solution. The number of collocation points, however, defines the length of control-variable vectors, which gets large enough to affect the efficiency of the SQP routine in obtaining the optimal solution. These issues restricted us to consider only the independently determined optimal temperature profiles in the case studies. The consequences of such limitations can be costly, especially when the current model is expanded to encompass interconnected subsystems comprising series of hy-

drocyclones for product classification and energy integration networks.

For the future, we suggest replacing the Lagrange basis function with the wavelet basis function for the purpose of reducing the length of control vectors. These bases are extremely effective in determining the coarseness of the discretization mesh according to the form of the function at a particular value of the independent variable. Their utility has been demonstrated through the solution of equations representing propagation of shock waves through fluids (Erlrebacher et al., 1996). Future work could also focus on developing mathematical relationships between PFR-type behavior and its possible counterparts in crystallization, such as draft-tube and column crystallizers. This would enable the extension of the networks to comprise different types of vessels, along with different operational schemes.

Acknowledgment

The authors are indebted to Dr. M. J. Hounslow of the University of Cambridge for helpful discussions on modeling stagewise particulate processes.

Notation

A = pre-exponential factor in nucleation rate expression, $cm^{-3} \cdot s^{-1}$
$\bar{A}$ = second moment of size distribution
B = nucleation rate, $cm^{-3} \cdot s^{-1}$
c = constant on nucleation-rate expression
G = crystal growth rate, $cm \cdot s^{-1}$
$f(\alpha)$ = fraction of crystals exiting CFR at point α
f_{ij} = fraction of crystals exiting discretized CFR at point α_{ij}
f_p = fraction of crystals obtained from the solution at pth iteration
f_r = linear combinator of concentrations from PFR section of recycle reactor
i, j, k = index of finite element i at collocation point j, k
J = objective function
k_g = growth-rate constant
$L_K(\alpha)$ = Lagrange interpolation polynomial of degree k
$L'_K(\alpha)$ = derivative of Lagrange interpolation polynomial
L = first moment of size distribution
n = number of crystals
$q(\alpha)$ = fraction of feed entering the system at point α
q_{ij} = fraction of feed entering discretized CFR at point α_{ij}
Q_0 = flow rate at the entry of the network
$Q(\alpha)$ = total flow rate at point α
$R(X)$ = reaction rate, s^{-1}
R_e = recycle ratio
s = supersaturation
$T(\alpha)$ = temperature at point α
X = dimensionless concentration
X_{ik} = dimensionless concentration at point i, k
$X_{i,\text{end}}$ = dimensionless concentration at the end of element i
X_0 = dimensionless concentration at network entry
α = time along the length of the network
$\Delta\alpha_i$ = length of finite element i
ϕ_i = ratio of feed flow to element i to bulk flow entering element i
τ = mean residence time, s

Literature Cited

Balakrishna, S., and L. T. Biegler, "Constructive Targeting Approach for the Synthesis of Chemical Reactors," *Ind. Eng. Chem. Res.*, **31**, 300 (1992a).

Balakrishna, S., and L. T. Biegler, "Targeting Strategies for the Synthesis and Energy Integration of Non-Isothermal Reactor Networks," *Ind. Eng. Chem. Res.*, **31**, 2152 (1992b).

Balakrishna, S., and L. T. Biegler, "Chemical Reactor Network Targeting and Integration: An Optimisation Approach," *Advances in Chemical Engineering*, J. L. Anderson, ed., Vol. 23, Academic Press, New York, p. 243 (1996).

Cuthrell, J. E., and L. T. Biegler, "On the Optimisation of Differential-Algebraic Process Systems," *AIChE J.*, **33**, 1257 (1987).

Doherty, M. F., "Pre-Synthesis Problem for Homogeneous Azeotropic Distillation Has a Unique Solution," *Chem. Eng. Sci.*, **40**, 1885 (1985).

Erlrebacher, G., M. Y. Hussaini, and L. M. Jameson, *Wavelets: Theory and Applications*, Oxford Univ. Press, New York (1996).

Garside, J., and R. J. Davey, "Secondary Contact Nucleation: Kinetics, Growth and Scale-Up," *Chem. Eng. Commun.*, **4**, 393 (1980).

Glasser, D., C. M. Crowe, and D. Hildebrandt, "A Geometric Approach to Steady Flow Reactors: The Attainable Region and Optimization in Concentration Space," *Ind. Eng. Chem. Res.*, **26**, 1803 (1997).

Helt, J. E., and M. A. Larson, "Effects of Temperature on the Crystallization of Potassium Nitrate by Direct Measurement of Supersaturation," *AIChE J.*, **23**, 822 (1977).

Hildebrandt, D., and L. T. Biegler, "Synthesis of Chemical Reactor Networks," *Foundations of Computer Aided Process Design (FOCAPD '94)*, L. T. Biegler and M. F. Doherty, eds., Snowmass, CO, p. 52 (1994).

Hill, P. J., and K. M. Ng, "Simulation of Solids Processes Accounting for Particle Size Distribution," *AIChE J.*, **43**, 715 (1997).

Hounslow, M. J., and E. J. W. Wynn, "Short-Cut Models for Particulate Processes," *Comput. Chem. Eng.*, **17**, 505 (1993).

Larson, M. A., and P. R. Wolff, "Crystal Size Distributions from Multistage Crystallizers," *Chem. Eng. Prog. Symp. Ser.*, **67**, 97 (1971).

Levenspiel, O., *Chemical Reaction Engineering*, Wiley, New York (1972).

Linhoff, B., and E. Hindmarsh, "The Pinch Design Method for Heat Exchanger Networks," *Chem. Eng. Sci.*, **38**, 745 (1983).

Listes, J. D., J. D. Smit, and M. J. Hounslow, "Adjustable Discretized Population for Growth and Aggregation," *AIChE J.*, **41**(3), 591 (1995).

Mullin, J. W., *Crystallization*, 3rd ed., Butterworth-Heinemann, Boston (1993).

Nývlt, J., *Design of Crystallizers*, CRC Press, Boca Raton, FL (1992).

Randolph, A. D., and C. Tan, "Numerical Design Techniques for Staged Classified Recycle Crystallizers: Examples of Continuous Alumina and Sucrose Crystallizers," *Ind. Eng. Process Des. Dev.*, **17**, 189 (1978).

Randolph, A. D., and M. A. Larson, *Theory of Particulate Processes*, 2nd ed., Academic Press, New York (1988).

Sheikh, A. Y., "Modelling, Synthesis, Optimisation and Control of Crystallization Processes," PhD Thesis, Univ. of London, London (1997).

Sheikh, A. Y., and A. G. Jones, "Crystallization Process Optimization via a Revised Machine Learning Methodology," *AIChE J.*, **43**(6), 1448 (1997).

Manuscript received Dec. 1, 1997, and revision received Mar. 23, 1998.